Endoplasmic reticulum stress does not contribute to steatohepatitis in obese and insulin resistant high-fat diet fed *foz/foz* mice

Vanessa Legry[1], Derrick M Van Rooyen[2], Barbara Lambert[1], Christine Sempoux[3], Laurence Poekes[1], Regina Español-Suñer[1], Olivier Molendi-Coste[1], Yves Horsmans[1], Geoffrey C Farrell[2], Isabelle A Leclercq[1]

[1]Laboratory of Hepato-Gastroenterology, Institut de Recherche Expérimentale et Clinique, Université catholique de Louvain (UCL), Brussels, Belgium
[2]Liver Research Group, ANU Medical School at The Canberra Hospital, Garran, ACT, Australia
[3]Pathology Department, St-Luc University Hospital, Université catholique de Louvain (UCL), Brussels, Belgium

Keywords: endoplasmic reticulum stress, non-alcoholic fatty liver disease, insulin resistance, apoptosis, inflammation

Short title: Endoplasmic reticulum stress in steatohepatitis

Number tables and Figures: 3 tables, 4 figures

Address for correspondence:
Correspondence should be addressed to Professor Isabelle Leclercq
Laboratoire d'Hépato-Gastro-Entérologie, Institut de Recherche Expérimentale et Clinique
Université catholique de Louvain
Avenue Mounier, 52 Box B1.52.01, B-1200 Brussels, Belgium
Phone : +32 2 764 52 73
Fax : +32 2 764 53 46
E-mail : isabelle.leclercq@uclouvain.be

List of Abbreviations:
Acc-1: acetyl-CoA carboxylase 1
Alms1: Alström syndrome 1
ALT: alanine transaminase
Atf4: activating transcription factor-4
Atf6: activating transcription factor-6
Bim: Bcl2-interacting mediator of cell death
BW: body weight
Chop: C/EBP homologous protein
Edem: ERAD enhancing mannosidase-like protein
eIF2α: eukaryotic initiation factor α
ER: endoplasmic reticulum
ERAD: ER-associated protein degradation
Fasn: fatty acid synthase
Gadd34: growth arrest DNA damage-34
Grp78: glucose regulated protein, 78 kDa
HFD: high-fat diet
Hsp90: heat shock protein 90
IR: insulin receptor
IRE1α: inositol-requiring-1α
JNK: c-jun N-terminal kinase
MCD: methionine- and choline- deficient

NAFLD: non-alcoholic fatty liver disease
NASH: non-alcoholic steatohepatitis
ND: normal diet
Nqo1: NAD(P)H dehydrogenase, quinone 1
PBA: phenyl-butyric acid
Pemt: phosphatidylethanolamine N-methyltransferase
PERK: protein kinase double-stranded RNA-dependent-like ER kinase
RT-qPCR: real time quantitative polymerase chain reaction
Scd-1: stearoyl-Coenzyme A desaturase 1
Srebp1c: sterol regulatory element binding protein-1c
Trib3: tribbles homolog 3
TUDCA: tauro-ursodeoxycholic acid
UPR: unfolded protein response
Xbp1: X-box binding protein 1

Abstract

Non-alcoholic fatty liver (steatosis) and steatohepatitis (NASH) are hepatic complications of metabolic syndrome. Endoplasmic reticulum (ER) stress is proposed as a crucial disease mechanism in obese and insulin resistant animals (such as *ob/ob* mice) with simple steatosis but its role in NASH remains controversial. We therefore evaluated the role of ER stress as a disease mechanism in *foz/foz* mice, which develop both the metabolic and the histological features that mimic human NASH.

We explored ER stress markers in the liver of *foz/foz* mice in response to high-fat diet (HFD) after several time points. We then evaluated the effect of treatment with ER stress inducer tunicamycin, or conversely with ER protectant tauro-ursodeoxycholic acid (TUDCA) on the metabolic and hepatic features.

Foz/foz mice are obese, glucose intolerant and develop NASH characterized by steatosis, inflammation, ballooned hepatocytes and apoptosis from 6 weeks of HFD feeding. This was not associated with activation of the upstream unfolded protein response (phospho-eIF2α, IRE1α activity, spliced Xbp1). Activation of JNK and up-regulation of Atf4 and Chop transcripts were however compatible with a "pathologic" response to ER stress. We tested it by intervention experiments. Induction of chronic ER stress failed to worsen obesity, glucose intolerance and NASH pathology in HFD-fed *foz/foz* mice. In addition, ER protectant TUDCA, although reducing steatosis, failed to improve glucose intolerance, hepatic inflammation and apoptosis in HFD-fed *foz/foz* mice.

These results show that signals driving hepatic inflammation, apoptosis and insulin resistance are independent of ER stress in obese, diabetic mice with steatohepatitis.

Introduction

Easy access to food in our modern societies has led to decreased physical activity and over-eating which dramatically increase the risks of obesity-related type 2 diabetes, cardiovascular and non-alcoholic fatty liver diseases (NAFLD). These conditions each have insulin resistance as a common denominator. In this metabolic context, several factors, among which hyperglycaemia, hyperinsulinemia, adipose inflammation and deregulated adipokine production pattern, digestive and gut-derived factors act to perturb liver lipid homeostasis leading to liver lipid accumulation [16;33]. In some patients, in addition to steatosis, hepatocellular injury and chronic inflammation develop, resulting in a progressive fibrotic disease termed non-alcoholic steatohepatitis (NASH).

The high protein synthesis capacity of hepatocytes requires a well-developed endoplasmic reticulum (ER). Various stress conditions, amongst which nutrient overload, oxidative stress, hypoxia or amino acid and glucose deprivation affect ER homeostasis and protein folding capacity. ER stress triggers the unfolded protein response (UPR) elements of which converge to increase folding capacity through chaperone production and reduction of protein loading through enhancing ER-associated protein degradation (ERAD) and attenuation of translation [27], thereby decreasing ER contrains. At a homeostatic state, the chaperone glucose-regulated protein 78 (Grp78/BiP) binds and blocks the activation of 3 ER trans-membrane proteins, i.e. inositol-requiring-1α (IRE1α), protein kinase double-stranded RNA-dependent-like ER kinase (PERK) and activating transcription factor-6 (Atf6) [9]. When misfolded or unfolded proteins accumulate in the ER, Grp78 releases those 3 sensors, leading to their activation. IRE1α, an endoribonuclease, splices X-box binding protein 1 (Xbp1) which stimulates the expression of Grp78 and ERAD enhancing mannosidase-like protein (Edem). PERK, via phosphorylation of eukaryotic translation initiation factor-2α subunit (eIF2α), globally inhibits protein translation. Active Atf6 translocates to the nucleus and enhances the transcription of genes encoding protein chaperones Grp78 and heat shock protein 90 (Hsp90/Grp94).

In addition to its primarily cytoprotective response, UPR has collateral side effects by inducing apoptosis, inflammation, insulin resistance and fat accumulation. Because of these deleterious consequences, it has been suggested that ER stress may participate to the development and propagation of NASH [3]. The ER stress pathologic response includes: enhanced expression and nuclear translocation of pro-apoptotic C/EBP homologous protein (Chop), induced mainly by PERK-dependent up-regulation of Atf4 transcription factor [29] but also by Atf6 and IRE1α pathways; PERK- and IRE1α-mediated induction of pro-inflammatory nuclear factor-κB; IRE1α-dependent activation of the c-Jun *N*-terminal kinase (JNK) which in turn impairs insulin signalling and can lead to apoptosis; PERK and Grp78-mediated activation of sterol regulatory element binding protein-1c (Srebp1c), the master regulator of *de novo* lipogenic program. In this way, the pathways activated during the response to ER stress could integrate lipid dysbiosynthesis, insulin resistance, inflammation and cell death in relation to excess cellular nutrient. It is therefore logical that ER stress has been envisaged as a pivotal pathogenic mechanism in NASH [3].

On the other hand, the evidence that ER stress mediates as opposed to accompanies development of fatty liver disease and transition to NASH is fragmentary. In the liver of leptin-deficient *ob/ob* mice, ER stress is evident and has been related to lipogenesis and hepatic insulin resistance [12;23]. However, ER stress does not necessarily accompany fatty liver disease in different genetic or diet-induced rodent models [38]. In humans, Puri *et al.* showed that, among the UPR markers, only phospho-eIF2α was increased in both NAFLD and NASH patients while the spliced form of XBP1 protein, found in controls and NAFLD, was low in NASH patients [25]. Gregor *et al.* showed that gastric bypass reduced phospho-eIF2α and Grp78 levels in liver and adipose tissue from obese patients, but data in liver were derived from only 4 liver biopsies [8]. Finally, Kumashiro *et al.* showed that in liver biopsies from 37 obese patients, ER stress markers correlated poorly with NAFLD-associated hepatic insulin resistance [13]. In summary, although several studies point to the UPR and

initiation of some ER stress signalling pathways in human and experimental NAFLD, mechanistic evidence that ER stress activates key pathogenic pathways in NASH is lacking.

We have used a metabolic syndrome model for NASH to clarify the operation and mechanistic significance of ER stress. Postnatally, *Alms1* mutant (*foz/foz)* mice lose hypothalamic neuronal cilia, location of key appetite sensing receptors, causing hyperphagic obesity with hyperleptinemia, hypoadiponectinemia and steatosis [11]. When fed a high fat diet, *foz/foz* mice rapidly develop obesity-related metabolic syndrome [2] and liver injury that recapitulates all the features of NASH: steatosis, liver inflammation, hepatocellular injury including ballooning and apoptotic cell death as well as progressive fibrosis [1]. We first measured expression of UPR and ER stress response proteins at various time points upon HFD feeding. In order to interrogate a causal relationship between ER stress response and liver pathology, we then performed interventions designed firstly to induce ER stress by a known mechanism (tunicamycin), and secondly to abrogate ER stress with the ER chaperone, tauro-ursodeoxycholic acid (TUDCA). Our data seriously challenge the notion that ER stress promotes the development of either the metabolic phenotype or steatohepatitis pathology in mice whose adipokine responses to obesity are the same as humans.

Material and methods

Animals and diets

Male *foz/foz* (*Alms1* mutant) NOD.B10 mice were bred and maintained in a 12-h light/dark cycle in the animal facility of Université catholique de Louvain (Brussels, Belgium). After weaning, mice were fed a standard rodent chow diet (ND) containing 2.83 kcal/g (16% fat, 54% carbohydrate, 30% protein, 0.001% cholesterol [wt/wt]; A03 from SAFE-diets, France) or a high-fat diet (HFD) which contains 5.24 kcal/g (60% fat, 20% carbohydrate, 20% protein, 0.03% cholesterol; D12492 from Research Diets, USA). Female WT and *foz/foz* mice were bred in the animal facility of ANU Medical School at The Canberra Hospital (Garran, ACT, Australia). All experiments were performed with approval of the local University Animal Welfare Committee.

Treatments

Male *foz/foz* mice were fed the ND or HFD for 3 days (5 mice per group), 6 weeks (≥ 5 mice per group) or 16 weeks (3 mice per group). Female WT and *foz/foz* mice were fed chow or HFD for 12 or 24 weeks (n=6 per group).

Tunicamycin (T7765 from Sigma) was dissolved at 200 µg/mL in 4.0% DMSO/10 mM Tris pH 8.0 [28]. Ten week-old male *foz/foz* mice under ND received an intraperitoneal (IP) injection of 1.0 mg/kg BW or an equivalent volume of diluent (6 mice per group) and were sacrificed 6 hours after treatment for the acute tunicamycin treatment. For chronic ER stress activation, another group of *foz/foz* mice were fed HFD for 5 weeks. After one week HFD feeding, an Alzet minipump (model 1004) loaded with tunicamycin or diluent was implanted in the inter scapulae subcutaneous tissue (5 per group) such as to obtain a continuous release of the product (10 ng/kg BW/day [17]) during 4 weeks. Mice were kept under HFD for the duration of treatment.

To inhibit ER stress, chemical chaperones were administered in a therapeutic setting. After 4 weeks HFD feeding in male *foz/foz* mice, treatment was initiated and repeated twice daily for 14 days. HFD was maintained during treatment. *Ob/ob* mice (7 week-old; Janvier, France) were used as a positive control and treated in parallel (same dose and simultaneously) with *foz/foz* mice. As chemical chaperones, we used 4-phenyl butyrate (PBA) in one hand and tauro-ursodeoxycholic acid (TUDCA) on the other. PBA was administered to mice (4 per group) by IP injection (water as vehicle) at the doses of 250 or 500 mg/kg twice a day (9 am and 6 pm, 0.5 or 1 g/kg BW/d).

Tauro-ursodeoxycholic acid (TUDCA) was administered to mice by IP injection (water as vehicle) at a dose of 250 mg/kg twice a day (9 am and 6 pm, 500 mg /kg BW/d). TUDCA treatment decreased food intake both in *ob/ob* and HFD-fed *foz/foz* mice (-7.6 kcal/day for both strains, $p<0.001$, n=3-4 per

group). Therefore, to clearly dissociate the effects of TUDCA from those due to decreased energy intake, mice were paired according to their body weight and glycaemia, and each control was pair-fed the same amount of food as that eaten by the corresponding TUDCA-treated mouse the day before (6-7 per group).
Please see supplementary experimental procedures.

Data analyses

Data are presented as means ± standard deviation (SD). Quantitative variables deviating from normal distribution were log-transformed. Differences between groups were analysed using the Student's t-test. Paired tests were performed between TUDCA-treated mice and their respective pair-fed controls. P values <0.05 were considered as statistically significant.

Results

High-fat diet-fed *foz/foz* mice develop metabolic and hepatic phenotypes similar to those encountered in human NASH

As previously reported, 6 weeks HFD induces obesity, adiposity and hepatomegaly in male *foz/foz* mice (Table 1). This was associated with fasting hyperglycaemia and pronounced glucose intolerance (Table 1, Figure 1 A). At this stage, liver histology showed macrovesicular steatosis with fat droplets present in more than 70% of hepatocytes (grade 3) (Figure 1 B). Biochemical analyses confirmed a 6-fold increase in hepatic lipids in HFD- versus ND-fed *foz/foz* mice (Table 1). Inflammatory foci were scattered through the parenchyma and hepatic F4/80 and CD68 transcript levels were significantly increased signifying macrophage activation (Figure 1 B & C). Ballooned hepatocytes were readily observed, as was hepatocellular apoptosis, indicated by the presence of apoptotic bodies and of M30-immunopositive hepatocytes (Figure 1 D). Elevated serum ALT level confirmed liver injury (Table 1). Thus, livers of HFD-fed *foz/foz* mice conform to all the criteria for a diagnosis of NASH. As reported elsewhere, upon continuation of HFD for longer period, severe fibrosing NASH will develop [1;15].

High-fat diet does not induce obvious ER stress in *foz/foz* mice

Compared to their ND-fed controls, we found no molecular signature of UPR in 6 week HFD-fed *foz/foz* livers: there was no increased phosphorylation of eIF2α or IRE1α upregulation, no splicing of Xbp1 and no increased expression of chaperones Grp78 and Hsp90 or upregulation of Edem (Figure 2 A-C). Also the expression of genes involved in *de novo* lipogenesis and phospholipid synthesis (Pemt) were not induced or rather reduced (Fasn, Scd-1) (Figure 2 D). This particularly contrasted with the *ob/ob* model which presented activation of the UPR and enhanced lipogenic genes expression, as already reported by others [12;23] (Supplementary Figure 1).
When activation of the UPR fails to restore homeostasis, the pro-apoptotic and pro-inflammatory pathways mentioned in the introduction prevail. As previously reported [14;35], JNK phosphorylation increased in HFD-fed *foz/foz* mouse livers compared to ND-fed counterparts (Figure 2 E). Further, Atf4 and Chop mRNA expression were significantly increased (Figure 2 F). However, nuclear Chop protein was not detectable (Figure 2 G) and only pro-apoptotic Bim was up-regulated but no other Chop targets such as Gadd34 or Trib3. This highly suggests that Chop does not mediate apoptosis in this model.
UPR activation was also investigated at different time points of HFD feeding. A short term HFD feeding (3 days) did not induce UPR in male *foz/foz* mice (Supplementary Figure 2 A-C). Also, UPR was not evidenced in *foz/foz* mice fed HFD for 16 weeks, which present a more advanced stage of steatohepatitis (Supplementary Figure 2 A-B-D). Finally, in female *foz/foz* mice which also develop NASH [15], there was also no up-regulation of Grp78 or nuclear Chop expression after 12 or 24 weeks of HFD feeding (Supplementary Figure 2 E-G).

Treatment with ER stress inducer does not aggravate metabolic and hepatic phenotype of HFD-fed *foz/foz* mice

Because of the theoretical concern that unidentified functions of Alms1 in the liver could alter a biological response such as ER stress, we sought to confirm that a known inducer of ER stress operated as anticipated in this line. Tunicamycin inhibits protein glycosylation leading to the accumulation of unfolded proteins in the ER lumen. As shown in Supplementary Figure 3, acute tunicamycin co-ordinately induced PERK-dependant eIF2α phosphorylation and Atf4/Chop expression and nuclear translocation, IRE1α expression and splicing of Xbp1, expression of chaperones and protein degradation machinery. However tunicamycin did not induce JNK phosphorylation in livers of *foz/foz* mice.

We then assessed whether prolonged ER stress activation would enhance metabolic disturbances and promote NASH in HFD-fed *foz/foz* mice. We therefore implanted tunicamycin-filled minipumps into HFD-fed *foz/foz* mice. Compared to vehicule-treated HFD-fed *foz/foz* controls, 4 weeks of tunicamycin infusion induced a UPR assessed by a significant increase in hepatic Grp78 and Hsp90 expression and in JNK phosphorylation (Figure 3 A-C). This was associated with decreased AKT phosphorylation on the threonine residue (Supplementary Figure 4 B). Despite this negative effect on insulin signalling pathway, chronic tunicamycin infusion did not further increase plasma glucose and c-peptide levels or glucose intolerance (Table 2 & Figure 3 E) in HFD-fed *foz/foz* mice. Similarly, it did not aggravate liver pathology. Thus, serum ALT levels and hepatic lipid content were similar in tunicamycin-treated and control HFD-fed *foz/foz* mice (Table 2). On histological examination (Figure 3 F and H), the degree of steatosis (52 ± 22% versus 32 ± 16% of fatty hepatocytes), the number of ballooned hepatocytes (1.8 ± 1.5 versus 1.3 ± 1.1 per high power field (20X), p=0.57) and the number of M30 positive hepatocytes (4.49 versus 2.73 per high power field, p=0.07) were not significantly different in tunicamycin- and PBS-treated HFD-fed *foz/foz* mice. Tunicamycin may have reduced the extent of inflammation, as reflected by the lower number of inflammatory foci compared to PBS-treated HFD-fed *foz/foz* mice (0.9 ± 0.6 versus 2 ± 0.7 per field (10X), p=0.003) with no significant change in F4/80 and CD68 mRNA expression (Figure 3 G).

The ER stress chaperone, tauro-ursodeoxycholic acid does not improve glucose tolerance or liver injury in HFD-fed *foz/foz* mice.

If ER stress always plays a role in the metabolic abnormalities of unhealthy obesity or in the pathogenesis of steatohepatitis, administration of agents that are known to abrogate an ER stress response should, at least partly, mitigate against these effects. Others have shown that the chemical chaperones 4-phenyl butyrate (PBA) and tauro-ursodeoxycholic acid (TUDCA) counteract ER stress and improve glucose homeostasis and steatosis in *ob/ob* mice [24]. We therefore examined the effects of these ER protectants in HFD-fed *foz/foz* mice and we used *ob/ob* mice as a positive control to validate the treatments. *Foz/foz* mice received PBA or TUDCA treatment during the last 2 weeks of a 6-week HFD feeding protocol. The chemical chaperone PBA which protected *ob/ob* mice against ER stress (data not shown) was highly toxic to *foz/foz* mice so that the mortality, which exceeded 70%, precluded interpretation. We then used TUDCA and observed that it reduced food intake (-7.6 kcal/day for both strains, p<0.001). Thus, we used pair-fed mice as controls to strictly dissociate any pharmacological effects of TUDCA from those attributable to decreased nutrient load. As expected, TUDCA treatment to *ob/ob* mice significantly improved steatosis and glucose homeostasis, and decreased the expression of UPR markers (Supplementary Figure 5). In HFD-fed *foz/foz* mice, the effect of TUDCA on ER homeostasis was confirmed by the decrease in eIF2α phosphorylation and IRE1α protein levels (Figure 4 A). This was associated with a further decrease in the expression of lipogenic genes (Figure 4 C) as well as Nqo1, a marker of oxidative stress (2-fold decrease, p=0.04). However, TUDCA treatment had no significant effect on JNK phosphorylation or on the expression of Chop and the target genes that were enhanced in HFD *foz/foz* livers (Figure 4 A & B).

At the physiological level, TUDCA treatment failed to decrease hyperglycaemia, serum c-peptide levels or to improve glucose tolerance and hepatic insulin signalling in HFD-fed *foz/foz* mice (Table 3, Figure 4 D and Supplementary Figure 3). TUDCA did reduce the severity of hepatic steatosis

histologically, and this effect was confirmed by a significant reduction in total hepatic lipid content (Table 3). However, TUDCA failed to reduce the number of inflammatory foci or the activation of Kupffer cells in the liver of HFD-fed *foz/foz* mice (Figure 4 E-F). Besides, ballooned hepatocytes were still readily observed in TUDCA-treated *foz/foz* livers and there was no improvement in M30 cytokeratin fragmentation immunostaining (Figure 4 G). We interpret these results as indicating that ER protectant, despite decreasing steatosis, does not improve glucose homeostasis, unlike in *ob/ob* mice, or the kind of liver injury that comprises transition to steatohepatitis in HFD-fed *foz/foz* mice.

Discussion

Perturbation in the normal function of the endoplasmic reticulum triggers a signalling network that coordinates adaptive, inflammatory and apoptotic responses. There is accumulating evidence implicating prolonged ER stress in the development and progression of many diseases, in particular in obesity-associated insulin resistance and NAFLD. A link between activation of the UPR and hepatic insulin resistance and steatosis has been demonstrated in *ob/ob* mice [12;23;24]. Increased eIF2α expression has been reported in human NASH livers [25], but with no evidence of aggravation in NASH livers compared to those with simple steatosis. Mice mutated for the ER secretory pathway protein, Sec61alpha1, develop hepatic steatosis, progressive liver injury with fibrosis when challenged with a HFD but intervention studies alleviating ER stress to test for causality were not reported [18].

To interrogate the participation of ER stress and UPR to obesity-associated liver injury, we used HFD-fed *foz/foz* mice which exhibit, in addition to steatosis, hepatic inflammation and hepatocellular injury that evolve with time into fully established NASH with typical perisinusoidal fibrosis [1;15]. If indeed a pathologic ER stress response develops, we reasoned that chemical induction of ER stress would worsen insulin resistance and apoptotic cell death. Conversely, ER protectants would have an opposite protective effect. Strikingly, tunicamycin-induced ER stress failed to significantly aggravate the metabolic and hepatic phenotype of HFD-fed *foz/foz* mice. Moreover, TUDCA, an ER protectant, despite decreasing steatosis, did not improve glucose homeostasis or liver injury in HFD-fed *foz/foz* mice. None of these findings provide support for the operation of ER stress in the pathophysiology and cellular pathology of insulin resistance-related steatohepatitis.

Among ER stress response markers, we found no signature of an adaptive response converging to reduce ER protein overload. Increased Atf4 and Chop transcripts and activation of JNK seen in HFD-fed *foz/foz* livers may be interpreted as part of an ER stress response. However, the causal relationship between those signalling events and UPR is not established in the absence of upstream activation of ER-transmembrane proteins. Further, disturbed ER homeostasis and UPR are not a unique mechanism converging to activate these factors. LPS, NO or oxidative stress [21;22] as well as DNA damage (chop is also known as Gadd153 -growth arrest and DNA damage inducible gene [6;30]) are potent stimuli for Chop up-regulation. Further analyses are needed to unravel the signals that up-regulate Chop expression in *foz/foz* mice. Importantly, increased Chop transcript, as it is not associated with increased nuclear translocation of the protein, is most likely irrelevant for inducing apoptosis in HFD-fed *foz/foz* livers.

The currently accepted model for JNK activation by free fatty acids involves ER stress through IRE1α [34]. Contradicting this paradigm, Sharma *et al.* showed that fatty acid-induced JNK activation was not inhibited in the absence of IRE1α and that fatty acid-induced cell death in hepatocytes was independent of IRE1α [31]. Therefore, the fact that JNK activation was observed in HFD-fed *foz/foz*

mice in the absence of IRE1α activation can readily be explained by the direct effects of lipotoxicity from accumulated free fatty acids [20] as well as free cholesterol (Gan and Van Rooyen 2013; unpublished data) rather than as part of a pathologic response to ER stress.

Despite the evident absence of ER stress in HFD-fed *foz/foz* mice, TUDCA treatment did reduce steatosis severity. In another genetic model of obesity, Yang *et al.* suggested that TUDCA improved hepatic steatosis by reducing oxidative stress [38]. Nqo1, a marker of oxidative stress, and several key lipogenic genes were decreased in TUDCA-treated *foz/foz* mice, supporting a role of oxidative stress in anti-steatotic effect of TUDCA. Furthermore, TUDCA, which is a hydrophilic bile acid, stimulates the synthesis and biliary secretion of phosphatidyl choline [19]. An increased fraction of hepatic free fatty acid may thus exit the liver as phospholipids and not participate to triglyceride synthesis, contributing to reduced steatosis.

As our results in *foz/foz* mice differ from those previously reported by elegant experimentation in other models, we consider that at least some of the earlier findings could be model-specific, many being in animals lacking leptin (*ob/ob* mice) [24] or a functional leptin receptor (*db/db* mice) [26]. To establish this we performed similar studies in *ob/ob* mice and were able to confirm the previously reported, adaptive response to ER stress in *ob/ob* livers and a beneficial effect of ER-protectants on steatosis and glucose homeostasis. Xu *et al* also reported differential effects of an ER protectant on glucose homeostasis in different models of type 2 diabetes: while PBA normalized hyperglycaemia in *ob/ob* mice, it had no glucose-lowering effect in Goto-Kakizaki rats and had no preventive or therapeutic effects on insulin resistance and hyperglycaemia in mice treated with hydrocortisone [37]. Therefore, the operation of ER stress could be related to the mechanisms causing metabolic alterations. Fu *et al.* demonstrated in *ob/ob* mice that lipogenesis, by altering the composition of ER membranes, causes the dysfunction of ER-anchored proteins and in particular that of the calcium pump SERCA resulting in modification of calcium fluxes impacting on protein folding capacity [7]. *De novo* lipogenesis is a prominent mechanism for steatosis in leptin-deficient mice [4;32]. This is not the case in obese humans with NAFLD [5], in which less than 30% of total hepatic lipid arises from hepatic lipogenesis, nor is it the case in *foz/foz* livers, in which steatosis results from increased delivery of fatty acid to the liver and altered lipid partitioning [14;15]; the latter finding is very similar to that observed by lipid turnover studies in humans [5].

In our study, TUDCA treatment did not have benefice on NASH progression. A similar observation was also reported by Henkel *et al.* applying TUDCA treatment in mice with MCD-induced steatohepatitis [10]. Noteworthy, the unconjugated form of this bile acid (UDCA) investigated for many years in the treatment for NASH is ineffective and cannot be recommended for NASH treatment [36]. Other non-UDCA bile acids, regulating metabolism by binding to the nuclear hormone receptor farnesoid X receptor and to a transmembrane bile acid receptor, TGR5, may deserve more attention.

In conclusion, this study shows that ER stress is not a feature associated with insulin resistance and steatohepatitis in the *foz/foz* model and that altering or protecting ER functions has no effect on insulin resistance and liver disease propagation. Data from earlier models may be model-specific. Since the progressive liver disease of the HFD-fed *foz/foz* mice, including hepatocellular injury with ballooning, apoptosis, inflammation and later accompanied with pericellular fibrosis, is more relevant to human NAFLD and NASH than is leptin-deficiency in *ob/ob* mice, convincing evidence gained from clinical studies would be required to provide support to the therapeutic effect of ER stress modifiers in human NASH.

Clinical Perspectives

Earlier studies have shown that counteracting ER stress using chemical chaperones such as TUDCA had a therapeutic benefit in obese and insulin resistant mouse models that develop simple steatosis. Using a unique model that develops the progressive liver disease in the metabolic context as seen in human NASH, we show that ER stress does not contribute to the pathogenesis of NASH and that TUDCA fails to alleviate glucose intolerance and hepatic inflammation and apoptosis, thus limiting the therapeutic potential of chemical chaperones to treat NASH.

Acknowledgements

The authors wish to thank Noémi Van Hul (UCL, Brussels Belgium), Sophie Lotersztajn INSERM U1149, Paris, France), and Peter L Jansen (University of Maastricht, The Netherlands) for their suggestions that enrich this manuscript.

Funding

The work was supported by grants from the D.G. Higher Education and Scientific Research of the French Community of Belgium, the Fund for Scientific Medical Research (Belgium), Australian National Health and Medical Research Council project grant 418101, and unrestricted research grants from AstraZeneca Belgium, Janssens Pharmaceutica Belgium, and Roche Belgium. IL is a FRS-FNRS research associate.

Reference List

1. Arsov,T., Larter,C.Z., Nolan,C.J., Petrovsky,N., Goodnow,C.C., Teoh,N.C., Yeh,M.M. and Farrell,G.C. (2006) Adaptive failure to high-fat diet characterizes steatohepatitis in Alms1 mutant mice. Biochem.Biophys.Res.Commun. **342**, 1152-1159.

2. Arsov,T., Silva,D.G., O'Bryan,M.K., Sainsbury,A., Lee,N.J., Kennedy,C., Manji,S.S., Nelms,K., Liu,C., Vinuesa,C.G., de Kretser,D.M., Goodnow,C.C. and Petrovsky,N. (2006) Fat aussie--a new Alstrom syndrome mouse showing a critical role for ALMS1 in obesity, diabetes, and spermatogenesis. Mol.Endocrinol. **20**, 1610-1622.

3. Dara,L., Ji,C. and Kaplowitz,N. (2011) The contribution of endoplasmic reticulum stress to liver diseases. Hepatology **53**, 1752-1763.

4. Dentin,R., Benhamed,F., Hainault,I., Fauveau,V., Foufelle,F., Dyck,J.R., Girard,J. and Postic,C. (2006) Liver-specific inhibition of ChREBP improves hepatic steatosis and insulin resistance in ob/ob mice. Diabetes **55**, 2159-2170.

5. Donnelly,K.L., Smith,C.I., Schwarzenberg,S.J., Jessurun,J., Boldt,M.D. and Parks,E.J. (2005) Sources of fatty acids stored in liver and secreted via lipoproteins in patients with nonalcoholic fatty liver disease. J.Clin.Invest **115**, 1343-1351.

6. Fornace,A.J., Jr., Nebert,D.W., Hollander,M.C., Luethy,J.D., Papathanasiou,M., Fargnoli,J. and Holbrook,N.J. (1989) Mammalian genes coordinately regulated by growth arrest signals and DNA-damaging agents. Mol.Cell Biol. **9**, 4196-4203.

7. Fu,S., Yang,L., Li,P., Hofmann,O., Dicker,L., Hide,W., Lin,X., Watkins,S.M., Ivanov,A.R. and Hotamisligil,G.S. (2011) Aberrant lipid metabolism disrupts calcium homeostasis causing liver endoplasmic reticulum stress in obesity. Nature **473**, 528-531.

8. Gregor,M.F., Yang,L., Fabbrini,E., Mohammed,B.S., Eagon,J.C., Hotamisligil,G.S. and Klein,S. (2009) Endoplasmic reticulum stress is reduced in tissues of obese subjects after weight loss. Diabetes **58**, 693-700.

9. Hendershot,L.M. (2004) The ER function BiP is a master regulator of ER function. Mt.Sinai J.Med. **71**, 289-297.

10. Henkel,A.S., Dewey,A.M., Anderson,K.A., Olivares,S. and Green,R.M. (2012) Reducing endoplasmic reticulum stress does not improve steatohepatitis in mice fed a methionine- and choline-deficient diet. Am.J.Physiol Gastrointest.Liver Physiol **303**, G54-G59.

11. Heydet,D., Chen,L.X., Larter,C.Z., Inglis,C., Silverman,M.A., Farrell,G.C. and Leroux,M.R. (2013) A truncating mutation of Alms1 reduces the number of hypothalamic neuronal cilia in obese mice. Dev.Neurobiol. **73**, 1-13.

12. Kammoun,H.L., Chabanon,H., Hainault,I., Luquet,S., Magnan,C., Koike,T., Ferre,P. and Foufelle,F. (2009) GRP78 expression inhibits insulin and ER stress-induced SREBP-1c activation and reduces hepatic steatosis in mice. J.Clin.Invest **119**, 1201-1215.

13. Kumashiro,N., Erion,D.M., Zhang,D., Kahn,M., Beddow,S.A., Chu,X., Still,C.D., Gerhard,G.S., Han,X., Dziura,J., Petersen,K.F., Samuel,V.T. and Shulman,G.I. (2011) Cellular mechanism of insulin resistance in nonalcoholic fatty liver disease. Proc.Natl.Acad.Sci.U.S.A **108**, 16381-16385.

14. Larter,C.Z., Yeh,M.M., Haigh,W.G., Van Rooyen,D.M., Brooling,J., Heydet,D., Nolan,C.J., Teoh,N.C. and Farrell,G.C. (2013) Dietary modification dampens liver inflammation and fibrosis in obesity-related fatty liver disease. Obesity.(Silver.Spring) **21**, 1189-1199.

15. Larter,C.Z., Yeh,M.M., Van Rooyen,D.M., Teoh,N.C., Brooling,J., Hou,J.Y., Williams,J., Clyne,M., Nolan,C.J. and Farrell,G.C. (2009) Roles of adipose restriction and metabolic factors in progression of steatosis to steatohepatitis in obese, diabetic mice. J.Gastroenterol.Hepatol. **24**, 1658-1668.

16. Leclercq,I.A. (2013) Emerging Concepts on the Pathogenesis on Non-Alcoholic Steatohepatitis (NASH). In Non-Alcoholoic Fatty Liver Disease: a Practical Guide (Farrell,G.C., McCullough,A.J. and Day,C.P., eds.), Wiley-Blackwell, Oxford, UK

17. Liang,B., Wang,S., Wang,Q., Zhang,W., Viollet,B., Zhu,Y. and Zou,M.H. (2013) Aberrant endoplasmic reticulum stress in vascular smooth muscle increases vascular contractility and blood pressure in mice deficient of AMP-activated protein kinase-alpha2 in vivo. Arterioscler.Thromb.Vasc.Biol. **33**, 595-604.

18. Lloyd,D.J., Wheeler,M.C. and Gekakis,N. (2010) A point mutation in Sec61alpha1 leads to diabetes and hepatosteatosis in mice. Diabetes **59**, 460-470.

19. Loria,P., Bozzoli,M., Concari,M., Guicciardi,M.E., Carubbi,F., Bertolotti,M., Piani,D., Nistri,A., Angelico,M., Romani,M. and Carulli,N. (1997) Effect of taurohyodeoxycholic acid on biliary lipid secretion in humans. Hepatology **25**, 1306-1314.

20. Malhi,H., Bronk,S.F., Werneburg,N.W. and Gores,G.J. (2006) Free fatty acids induce JNK-dependent hepatocyte lipoapoptosis. J.Biol.Chem. **281**, 12093-12101.

21. Nakayama,Y., Endo,M., Tsukano,H., Mori,M., Oike,Y. and Gotoh,T. (2010) Molecular mechanisms of the LPS-induced non-apoptotic ER stress-CHOP pathway. J.Biochem. **147**, 471-483.

22. Oyadomari,S. and Mori,M. (2004) Roles of CHOP/GADD153 in endoplasmic reticulum stress. Cell Death.Differ. **11**, 381-389.

23. Ozcan,U., Cao,Q., Yilmaz,E., Lee,A.H., Iwakoshi,N.N., Ozdelen,E., Tuncman,G., Gorgun,C., Glimcher,L.H. and Hotamisligil,G.S. (2004) Endoplasmic reticulum stress links obesity, insulin action, and type 2 diabetes. Science **306**, 457-461.

24. Ozcan,U., Yilmaz,E., Ozcan,L., Furuhashi,M., Vaillancourt,E., Smith,R.O., Gorgun,C.Z. and Hotamisligil,G.S. (2006) Chemical chaperones reduce ER stress and restore glucose homeostasis in a mouse model of type 2 diabetes. Science **313**, 1137-1140.

25. Puri,P., Mirshahi,F., Cheung,O., Natarajan,R., Maher,J.W., Kellum,J.M. and Sanyal,A.J. (2008) Activation and dysregulation of the unfolded protein response in nonalcoholic fatty liver disease. Gastroenterology **134**, 568-576.

26. Rinella,M.E., Siddiqui,M.S., Gardikiotes,K., Gottstein,J., Elias,M. and Green,R.M. (2011) Dysregulation of the unfolded protein response in db/db mice with diet-induced steatohepatitis. Hepatology **54**, 1600-1609.

27. Ron,D. and Walter,P. (2007) Signal integration in the endoplasmic reticulum unfolded protein response. Nat.Rev.Mol.Cell Biol. **8**, 519-529.

28. Schaap,F.G., Kremer,A.E., Lamers,W.H., Jansen,P.L. and Gaemers,I.C. (2013) Fibroblast growth factor 21 is induced by endoplasmic reticulum stress. Biochimie **95**, 692-699.

29. Scheuner,D., Song,B., McEwen,E., Liu,C., Laybutt,R., Gillespie,P., Saunders,T., Bonner-Weir,S. and Kaufman,R.J. (2001) Translational control is required for the unfolded protein response and in vivo glucose homeostasis. Mol.Cell **7**, 1165-1176.

30. Schmitt-Ney,M. and Habener,J.F. (2000) CHOP/GADD153 gene expression response to cellular stresses inhibited by prior exposure to ultraviolet light wavelength band C (UVC). Inhibitory sequence mediating the UVC response localized to exon 1. J.Biol.Chem. **275**, 40839-40845.

31. Sharma,M., Urano,F. and Jaeschke,A. (2012) Cdc42 and Rac1 are major contributors to the saturated fatty acid-stimulated JNK pathway in hepatocytes. J.Hepatol. **56**, 192-198.

32. Shimomura,I., Bashmakov,Y. and Horton,J.D. (1999) Increased levels of nuclear SREBP-1c associated with fatty livers in two mouse models of diabetes mellitus. J.Biol.Chem. **274**, 30028-30032.

33. Tilg,H. and Moschen,A.R. (2010) Evolution of inflammation in nonalcoholic fatty liver disease: the multiple parallel hits hypothesis. Hepatology **52**, 1836-1846.

34. Urano,F., Wang,X., Bertolotti,A., Zhang,Y., Chung,P., Harding,H.P. and Ron,D. (2000) Coupling of stress in the ER to activation of JNK protein kinases by transmembrane protein kinase IRE1. Science **287**, 664-666.

35. Van Rooyen,D.M., Gan,L.T., Yeh,M.M., Haigh,W.G., Larter,C.Z., Ioannou,G., Teoh,N.C. and Farrell,G.C. (2013) Pharmacological cholesterol lowering reverses fibrotic NASH in obese, diabetic mice with metabolic syndrome. J.Hepatol. **59**, 144-152.

36. Wu,S.D., Li,L. and Wang,J.Y. (2012) Ursodeoxycholic acid for nonalcoholic steatohepatitis. Eur.J.Gastroenterol.Hepatol. **24**, 1247-1253.

37. Xu,T.Y., Chen,R.H., Wang,P., Zhang,R.Y., Ke,S.F. and Miao,C.Y. (2010) 4-Phenyl butyric acid does not generally reduce glucose levels in rodent models of diabetes. Clin.Exp.Pharmacol.Physiol **37**, 441-446.

38. Yang,J.S., Kim,J.T., Jeon,J., Park,H.S., Kang,G.H., Park,K.S., Lee,H.K., Kim,S. and Cho,Y.M. (2010) Changes in hepatic gene expression upon oral administration of taurine-conjugated ursodeoxycholic acid in ob/ob mice. PLoS.One. **5**, e13858.

Figure legends

Figure 1: High-fat diet-fed *foz/foz* mice present all the metabolic and histologic features of human NASH

(A) Curves of glycaemia during intra-peritoneal glucose tolerance test and area under the glucose curves (AUC) in *foz/foz* mice fed normal diet (ND-plain forms) or high-fat diet (HFD-open forms) during 6 weeks. (B) Haematoxylin and eosin staining of liver sections showing steatosis in HFD-fed *foz/foz* mice compared to ND (original magnification X10). Higher magnification figures (X20) highlight ballooned hepatocytes (arrows, a), mitosis (b), nuclear glycogen inclusion (c), apoptotic body (d) and inflammatory infiltrates (e) in HFD *foz/foz* livers. (C) F4/80 and CD68 mRNA levels assessed by reverse transcription and real time PCR on whole liver RNA. (D) Immunohistochemistry using antibody against cleaved cytokeratin 18 (M30) demonstrating apoptotic hepatocytes in HFD *foz/foz* livers (original magnification X20). **p*<0.05

Figure 2: Adaptive and pathologic ER stress responses in *foz/foz* mice

RNA and total proteins were extracted from livers of normal diet (ND or plain bars) or high-fat diet-fed *foz/foz* mice (HFD or open bars) to evaluate (A) eIF2α phosphorylation (parts of the same immunoblot) and IRE1α protein levels by western blot (left panel) and quantification (right panel); (B) Xbp1 splicing by reverse transcription PCR (products loaded on agarose gel; spliced=147 bp, unspliced=173 bp; T, positive control with tunicamycin); (C) expression of target genes of adaptive UPR by RT-qPCR; (D) expression of lipogenic genes measured by RT-qPCR; (E) phosphorylation of JNK by western blot (parts of the same immunoblot) and quantification; (F) expression of target genes of pathologic ER stress response by RT-qPCR; (G) nuclear Chop protein level assessed by western blot. **p*<0.05

Figure 3: Chronic activation of ER stress does not worsen *foz/foz* phenotype

(A) Quantification of eIF2α and JNK phosphorylation and IRE1α protein levels assessed by western blot, (B) expression of adaptive and pathologic ER stress response target genes assessed by RT-qPCR, (C) Xbp1 splicing, (D) expression of lipogenic genes measured by RT-qPCR, (E) IP glucose tolerance test (area under the curves p=0.15), (F) Haematoxylin and eosin staining of liver sections (10X magnification), (G) expression of F4/80 and CD68 mRNA assessed by RT-qPCR and (H) quantification of apoptotic cells stained using M30 antibody for cleaved cytokeratin 18 in 5 weeks HFD-fed *foz/foz* mice treated for 4 weeks with tunicamycin (TUN or hatched bars) or not (CTL or open bars). **p*<0.05

Figure 4: TUDCA decreases UPR and steatosis but fails to reduce JNK and Chop and to improve glucose intolerance, hepatic insulin signalling, inflammation and apoptosis in HFD-fed *foz/foz* mice

RNA and total proteins were extracted from whole livers of 6 week HFD-fed *foz/foz* mice that received TUDCA IP injections for the last 2 weeks (TUDCA or dotted bars) and pair-fed controls (pair-fed or open bars). (A) Quantification of eIF2α and JNK phosphorylation and IRE1α protein levels assessed by western blot. (B) Expression of adaptive and pathologic ER stress response target genes assessed by RT-qPCR. (C) Expression of lipogenic genes measured by RT-qPCR. (D) IP glucose tolerance test (area under the curves *p*=0.92). (E) Haematoxylin and eosin staining (left panels) and F4/80 immunohistochemistry (right panels) of the liver sections (10X magnification). (F) Expression of F4/80 and CD68 assessed by RT-qPCR. (G) Quantification of apoptotic cells stained using M30 antibody for cleaved cytokeratin 18. **p*<0.05

583 **Tables**

584

585 Table 1: Metabolic parameters in *foz/foz* mice fed normal diet (ND) or high-fat diet (HFD) for 6 weeks
586 after weaning

587

	ND	**HFD**	***p* value**
n	5	9	
Body weight (g)	22.5 ± 1.9	48.7 ± 2.6	2.10^{-10}
Liver weight (g)	1.31 ± 0.19	2.64 ± 0.42	3.10^{-6}
Liver/body (%)	5.81 ± 0.51	5.40 ± 0.65	0.22
Hepatic lipid content (mg/100mg tissue)	7.36 ± 3.68	43.08 ± 13.82	9.10^{-5}
Epididymal adipose tissue weight (g)	0.32 ± 0.13	2.71 ± 0.31	2.10^{-10}
Epididymal adipose tissue/body (%)	1.41 ± 0.55	5.60 ± 0.81	2.10^{-7}
Fasting glycaemia (mg/dL)	148 ± 21	229 ± 9	0.03
Insulin C-peptide (pM)	1652 ± 1079	2552 ± 1529	0.15
Alanine aminotransferase (IU/L)	50.3 ± 6.9	108.0 ± 55.2	0.02
Total caloric intake (kcal/day)	8.33 ± 0.58	17.85 ± 2.98	0.0002
Caloric intake from fat (kcal/day)	1.33 ± 0.09	10.71 ± 1.79	0.00002

588

589

590
591 Table 2: Metabolic parameters in high-fat diet-fed *foz/foz* mice treated or not with tunicamycin in a
592 chronic setting
593

	Control	**Tunicamycin**	***p* value**
n	5	5	
Body weight (g)	38.0 ± 3.9	36.0 ± 5.22	0.30
Body weight gain (g)	+ 17.7 ± 3.0	+ 19.2 ± 2.4	0.41
Liver weight (g)	2.24 ± 0.52	2.33 ± 0.50	0.79
Hepatic lipid content (mg/100mg tissue)	38.52 ± 10.73	28.88 ± 10.01	0.18
Epididymal adipose tissue weight (g)	2.01 ± 0.43	2.40 ± 0.59	0.28
Fasting glycaemia (mg/dL)	224 ± 49	239 ± 73	0.71
Insulin C-peptide (pM)	1345 ± 178	1464 ± 554	0.67
Alanine aminotransferase (IU/L)	106.0 ± 28.3	120.3 ± 40.4	0.67

594
595

Table 3: Metabolic parameters in high-fat diet-fed *foz/foz* mice treated or not with TUDCA

	pairfed control	**TUDCA**	***p* value**
n	7	6	
Body weight (g)	36.9 ± 4.6	36.0 ± 5.22	0.77
Liver weight (g)	1.68 ± 0.26	1.43 ± 0.09	0.046
Liver/body (%)	4.54 ± 0.27	4.02 ± 0.42	0.031
Hepatic lipid content (mg/100mg tissue)	20.6 ± 4.5	13.2 ± 3.3	0.006
Epididymal adipose tissue weight (g)	2.13 ± 0.50	1.82 ± 0.53	0.30
Fasting glycaemia (mg/dL)	201 ± 41	171 ± 35	0.21
Insulin C-peptide (pM)	634 ± 278	558 ± 101	0.55

Summary statement

Unlike in mice developing simple steatosis, endoplasmic reticulum stress does not contribute to the pathogenesis of insulin resistance and steatohepatitis in high-fat diet-fed *foz/foz* mice, which develop the progressive liver disease in the metabolic context seen in human non-alcoholic steatohepatitis.

Author contribution

V Legry: conception and design of the study, generation, analysis and interpretation of data, and writing the manuscript; DM Van Rooyen: design of the study, generation and analysis of data; B Lambert: generation and collection of data; C Sempoux: histological analyses and data interpretation; L Poekes: generation and collection of data; R Español-Suñer: generation and collection of data and revision of the manuscript; O Molendi-Coste: generation and collection of data; Y Horsmans: interpretation of data, and revision the manuscript; GC Farrell: conception and design of the study, and revision of the manuscript; IA Leclercq: conception, design and supervision of the study, and writing the manuscript.

Figure 1

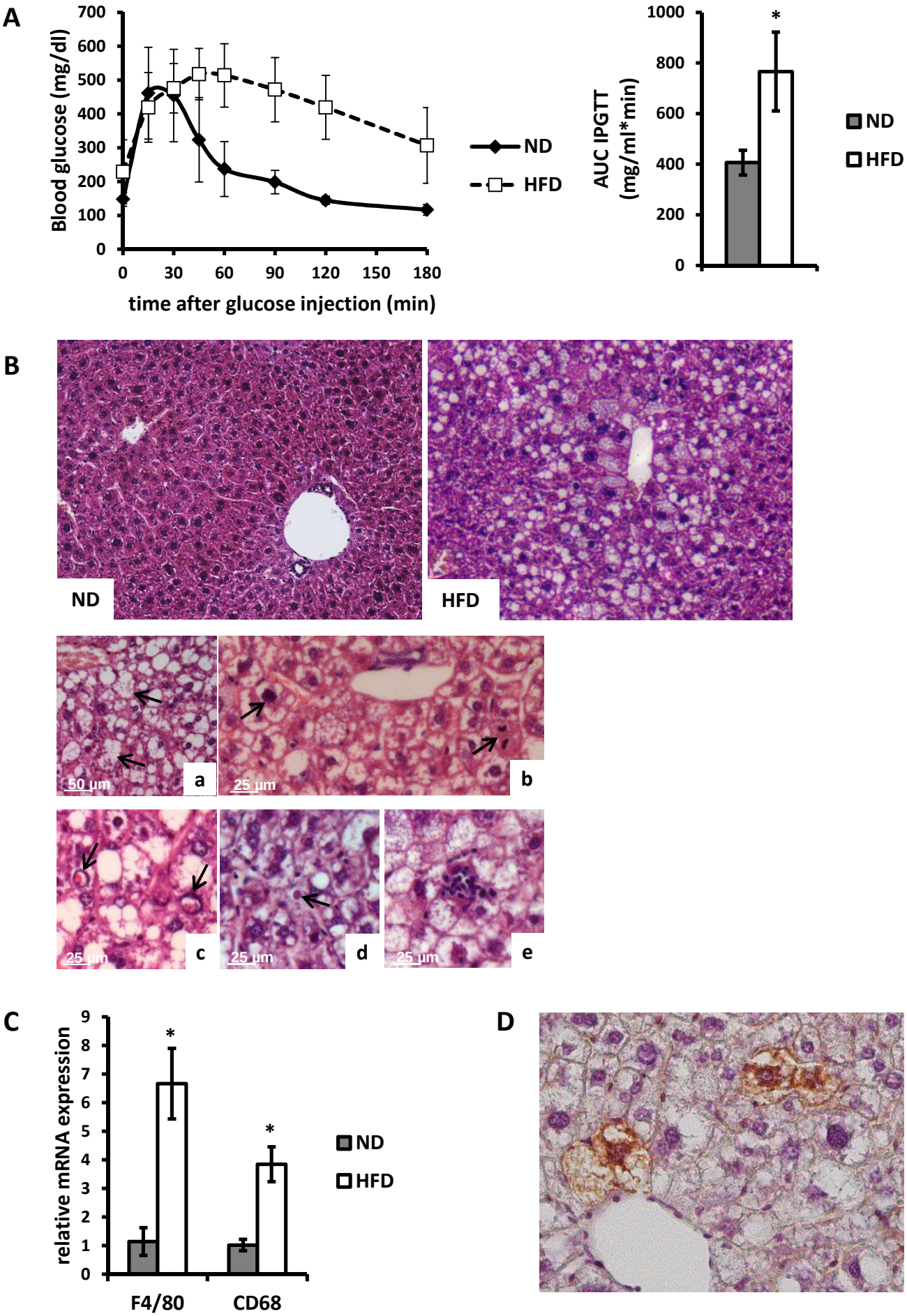
A
Blood glucose (mg/dl)
700
600
500
400
300
200
100
0
0
30
60
90
120
150
180
time after glucose injection (min)
ND
HFD
AUC IPGTT (mg/ml*min)
1000
800
600
400
200
0
*
ND
HFD
B
ND
HFD
50 µm
a
25 µm
b
25 µm
c
25 µm
d
25 µm
e
C
relative mRNA expression
9
8
7
6
5
4
3
2
1
0
*
*
F4/80
CD68
ND
HFD
D

Figure 2

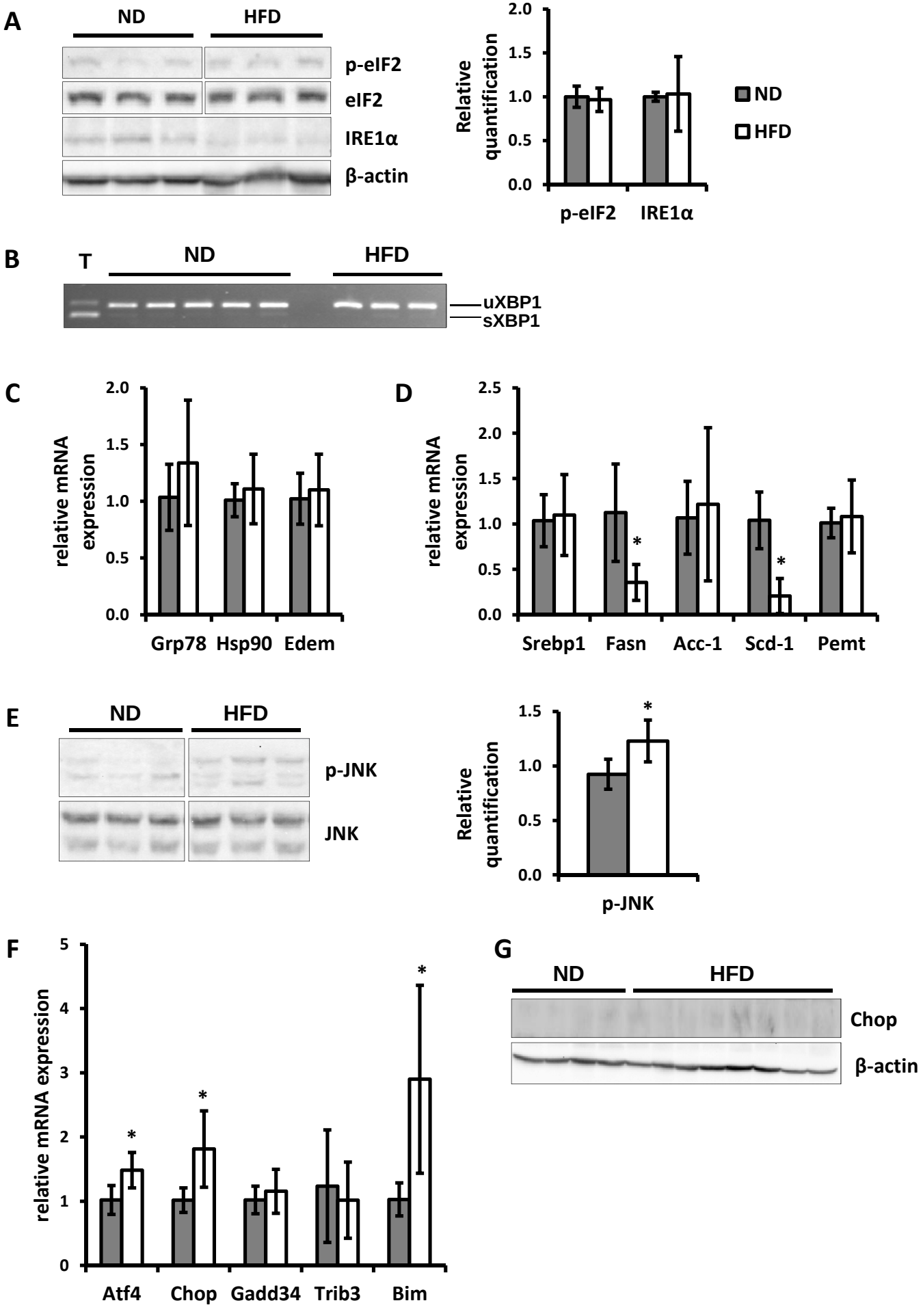
A
ND
HFD
p-eIF2
eIF2
IRE1α
β-actin
Relative quantification
2.0
1.5
1.0
0.5
0.0
ND
HFD
p-eIF2
IRE1α
B
T
ND
HFD
uXBP1
sXBP1
C
relative mRNA expression
2.0
1.5
1.0
0.5
0.0
Grp78
Hsp90
Edem
D
relative mRNA expression
2.5
2.0
1.5
1.0
0.5
0.0
*
*
Srebp1
Fasn
Acc-1
Scd-1
Pemt
E
ND
HFD
p-JNK
JNK
Relative quantification
1.5
1.0
0.5
0.0
*
p-JNK
F
relative mRNA expression
5
4
3
2
1
0
*
*
*
Atf4
Chop
Gadd34
Trib3
Bim
G
ND
HFD
Chop
β-actin

Figure 3

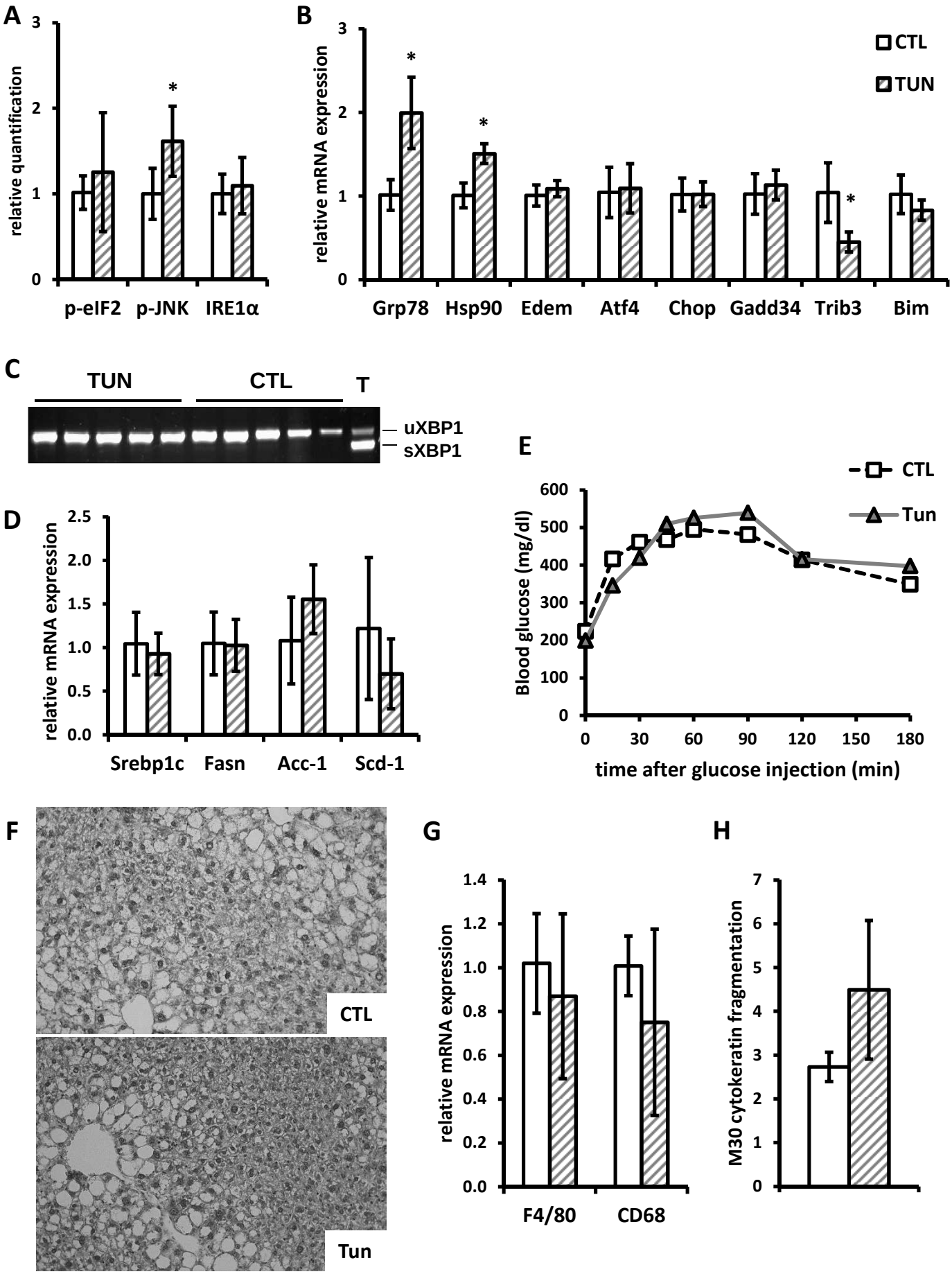
A
relative quantification
p-eIF2
p-JNK
IRE1α
B
relative mRNA expression
CTL
TUN
Grp78
Hsp90
Edem
Atf4
Chop
Gadd34
Trib3
Bim
C
TUN
CTL
T
uXBP1
sXBP1
D
relative mRNA expression
Srebp1c
Fasn
Acc-1
Scd-1
E
CTL
Tun
Blood glucose (mg/dl)
time after glucose injection (min)
F
CTL
Tun
G
relative mRNA expression
F4/80
CD68
H
M30 cytokeratin fragmentation

Figure 4

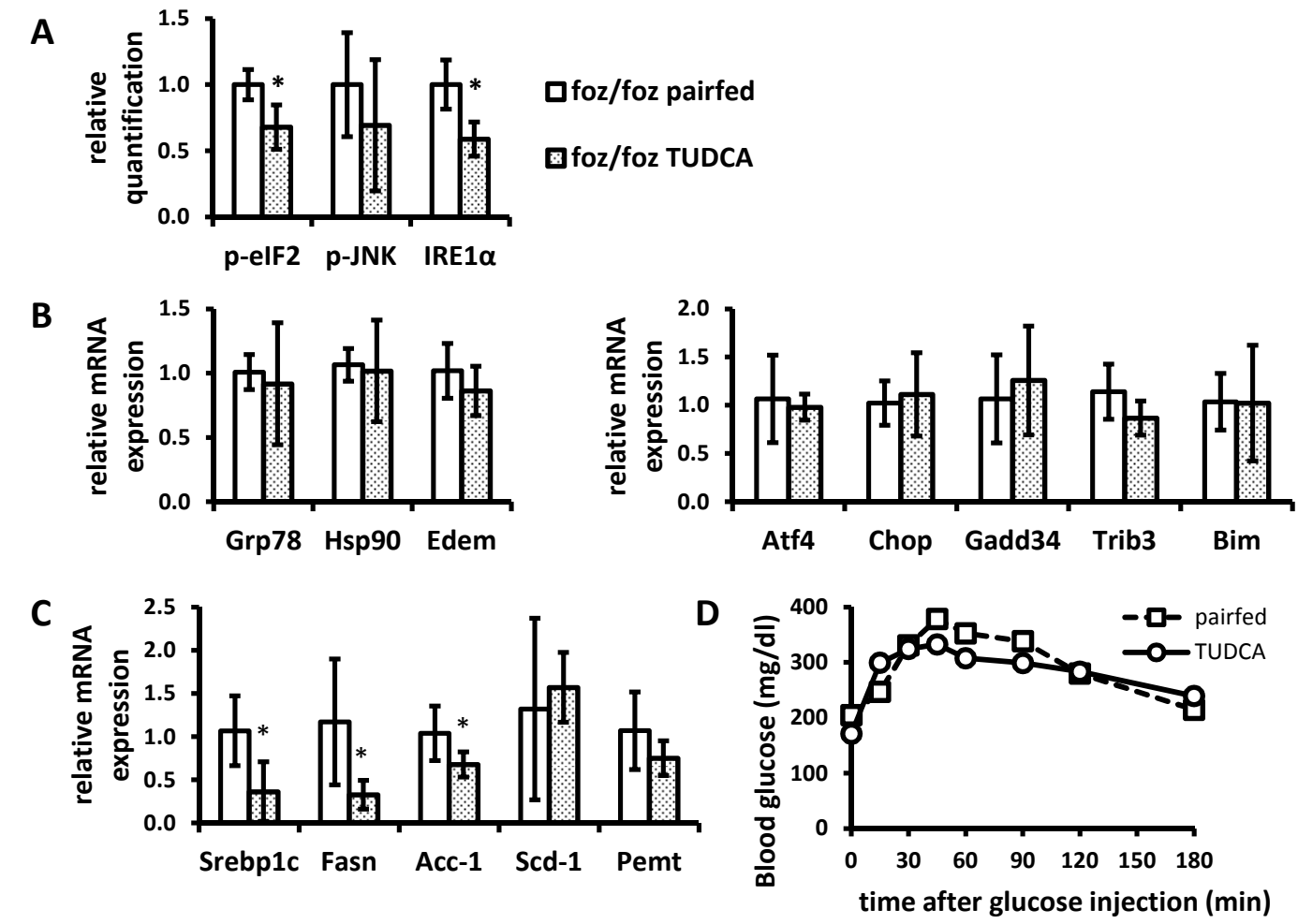
A
relative quantification
1.5
1.0
0.5
0.0
*
*
p-eIF2
p-JNK
IRE1α
foz/foz pairfed
foz/foz TUDCA
B
relative mRNA expression
Grp78
Hsp90
Edem
Atf4
Chop
Gadd34
Trib3
Bim
C
Srebp1c
Fasn
Acc-1
Scd-1
Pemt
D
Blood glucose (mg/dl)
400
300
200
100
0
0
30
60
90
120
150
180
time after glucose injection (min)
pairfed
TUDCA

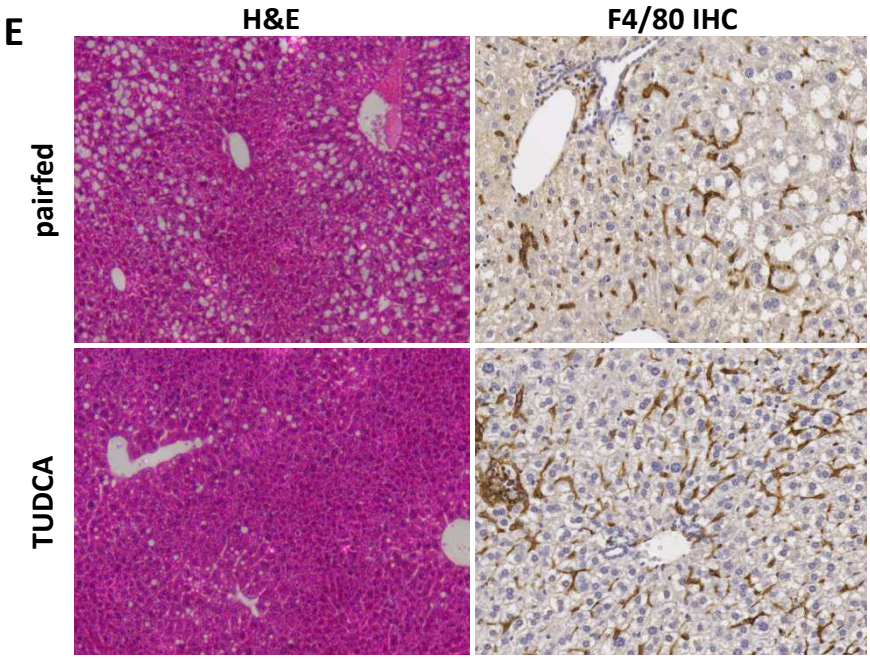
E
H&E
F4/80 IHC
pairfed
TUDCA

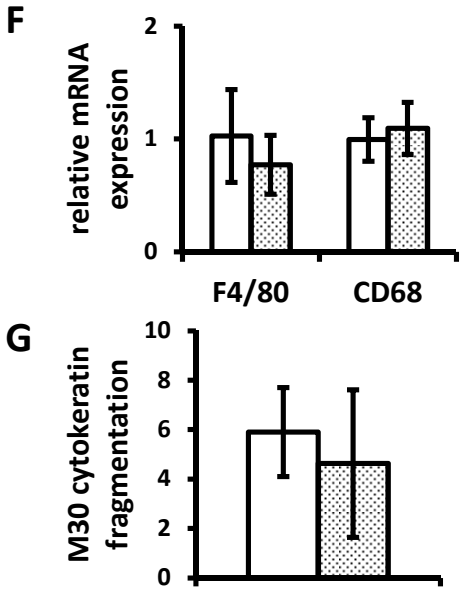
F
relative mRNA expression
2
1
0
F4/80
CD68
G
M30 cytokeratin fragmentation
10
8
6
4
2
0

Supplementary material

Material and methods

Animals and treatment

Six week-old male *ob/ob* mice and their lean (*ob/+*) littermates were purchased from Janvier (France), fed chow and maintained in the animal facility of Université catholique de Louvain (Brussels, Belgium) for 3 weeks. Treatment was initiated after 1 week acclimation.

At the time of sacrifice, anesthetized (ketamine/xylazine) mice received 5 U insulin (Actrapid, Novo Nordisk, Bagsvaerd, Denmark) or an equal volume of PBS into the portal vein to analyse the intrahepatic response to insulin. The liver was removed 1 min after the injection, and epididymal adipose tissue were dissected and weighed. Portions of tissue were immersed in formalin 4% for histology; the remaining tissue was snap frozen in liquid nitrogen and kept at -80°C until analyses.

Histology and immunohistochemistry

Formalin-fixed, paraffin-embedded sections were used for histological evaluation with haematoxylin and eosin (H&E) staining. Steatosis was estimated by counting the number of fatty hepatocytes in relation to the total number of hepatocytes and expressed as percentage of steatosis. Quantification has been performed on minimum 8 fields (objective 10X, magnification 100X).

Tissue sections underwent antigen retrieval (sodium citrate) and antibody labelling. F4/80 was detected using a primary rat anti-mouse F4/80 monoclonal antibody (1/200, Serotec, Oxford, UK), a rabbit anti-rat immunoglobulin (1/200, Dako, Glostrup, Denmark) and then a goat anti-rabbit streptavidin horseradish peroxidase conjugated antibody (En Vision, Dako). Cleaved cytokeratine 18 (M30 epitope) was detected using a primary mouse antibody (1/100, Roche) and the MOM kit according to the manufacturer recommendations (Dako). The peroxidase activity was revealed with diaminobenzidine and slides were counterstained with haematoxylin. Quantification was performed in a minimum of 5 random 20X-power fields per section.

Glucose homeostasis assessment

Blood was retrieved from the tail vein on 4-hours fasted mice and used to measure glucose (Accu-chek Aviva; Roche) and C-peptide plasma concentration using an enzyme immunoassay (ALPCO, USA).

To evaluate glucose tolerance, glucose (1 g/kg body weight) was injected IP after a fasting period of 4 hours, and glucose levels were monitored in tail blood at 0, 15, 30, 60, 90, 120 and 180 min after the injection. Glucose tolerance test was performed 2 days prior to sacrifice, or after 12 days of TUDCA, PBA or vehicle treatment.

Lipid and protein analyses

Total liver lipids were extracted with methanol and chloroform and quantified using the vanillin phosphoric acid reaction [1]. To analyse the ER stress response, proteins from liver homogenates (100 µg) were assayed by western blotting using the antibodies and conditions listed in Supplementary Table 1. Immunoreactivity was detected with a horseradish peroxidase-conjugated secondary antibody and enhanced chemiluminescence reagents (Western Lightning Chemiluminescence Reagent Plus; Perkin Elmer). One membrane was sequentially probed with the antibodies against the total protein, the phospho-protein, and GAPDH or beta-actin to control for protein loading. The quantification of immunoreactive proteins was obtained by densitometry using the Gel DocTM XR System 170–8,170 device and software (Bio-Rad). The levels of immunoreactivity relative to the invariant control are reported as arbitrary densitometry units. Phosphorylation was estimated by calculating the ratio of phospho-protein divided by the total form of the protein.

RNA extraction, reverse transcription and real time quantitative PCR (RT-qPCR)

Total RNA was extracted from frozen liver using TRIpure Isolation Reagent (Roche Diagnostics Belgium, Vilvoorde, Belgium). cDNA was synthesized from 1 µg RNA using random primers and M-MLV RT (Invitrogen, Merelbeke, Belgium). Real-time PCR analysis was performed as described previously [1]. Primer pairs for transcripts of interest were designed using the Primer Express design software (Applied Biosystems, Belgium) and are listed in Supplementary Table 2. RPL19 mRNA was chosen as an invariant standard. All experimental tissues and standard curve samples were run in duplicate in a 96-well reaction plate (MicroAmp Optical; Applied Biosystems). Results are expressed as fold expression relative to expression in the control group using the ΔΔCt method [1].

Supplementary Figure legends

Supplementary Figure 1: Comparison of ER stress response between *foz/foz* and *ob/ob* models
RNA and total proteins were extracted from whole livers of 9 week-old *ob/ob* mice (pale grey bars), their lean littermates (white bars) and *foz/foz* mice fed normal diet (foz+ND or dark grey bars) or high-fat diet (foz+HFD or hatched bars) for 6 weeks. (A) Quantification of eIF2α phosphorylation and IRE1α protein expression assessed by western blot. (B) Expression of UPR target genes assessed by RT-qPCR. (C) Expression of lipogenic genes measured by RT-qPCR. * p<0.05 *ob/ob* vs. lean. † p<0.05 *foz*+HFD vs. *ob/ob*. ¥ p<0.05 *foz*+HFD vs. *foz*+ND

Supplementary Figure 2: ER-stress response in male (A-D) and female (E-G) *foz/foz* mice at different time points of HFD feeding
RNA and total proteins were extracted from livers of male *foz/foz* mice after 3 days and 16 weeks of HFD to evaluate (A) eIF2α phosphorylation by western blot, (B) Xbp1 splicing, (C-D) expression of UPR target genes by RT-qPCR. (E) Grp78 protein, (F) Chop mRNA and (G) nuclear protein expression at 12 and 24 weeks in female WT and *foz/foz* mice fed chow or HFD. * p <0.05, vs diet-matched control. #p<0.05, vs genotype-matched control.

Supplementary Figure 3: ER-stress response induced by tunicamycin in *foz/foz* mice
ND-fed *foz/foz* mice were treated with tunicamycin 1.0 mg/kg BW, IP (Tun, hatched bars) or vehicle (ND, plain bars) and the liver analysed 6 hours later. (A) eIF2α phosphorylation and IRE1α protein levels assessed by western blot (left panel) and quantification (right panel); (B) XBP1 splicing; (C) expression of target genes of adaptive UPR by RT-qPCR; (D) phosphorylation of JNK and nuclear Chop protein level assessed by western blot; (E) expression of pro-apoptotic UPR target genes measured by RT-qPCR. *p<0.05

Supplementary Figure 4: Hepatic insulin signaling in *foz/foz* mice
Insulin sensitivity was evaluated by phosphorylation of signalling intermediates (p-IR on Tyr1162/1163, p-AKT on Ser473 and on Thr308) upon insulin stimulus as determined by western blot in (A) *foz/foz* mice fed ND or HFD for 6 weeks, (B) 5 weeks HFD-fed *foz/foz* mice treated for 4 weeks with tunicamycin (TUN) or not (CTL) and (C) 6 week HFD-fed *foz/foz* mice that received TUDCA IP injections for the last 2 weeks (+TUDCA) and pair-fed HFD controls (-TUDCA).

Supplementary Figure 5: Side by side comparison of TUDCA effect in *ob/ob* and *foz/foz* models
4 week HFD-fed *foz/foz* mice and chow-fed *ob/ob* mice received simultaneously TUDCA IP injections during 2 weeks (TUDCA or dotted bars). Pair-fed controls (pair-fed or open bars) received PBS IP injections. RNA and total proteins were extracted from whole livers. (A) Quantification of eIF2α and JNK phosphorylation and IRE1α protein expression assessed by western blot. (B) Expression of UPR target genes assessed by RT-qPCR. (C) Expression of lipogenic genes measured by RT-qPCR. (D) IP glucose tolerance test (area under the curves p=0.92 for *foz/foz* mice TUDCA vs. pair-fed; p=0.05 for

ob/ob mice TUDCA vs. pair-fed). (E) Haematoxylin and eosin staining of the liver sections (10X magnification). *p<0.05 TUDCA vs. respective pair-fed controls

Supplementary Table 1: List of the antibodies used in western blotting

Protein	**Epitope**	**# Antibody**	**Isotype**	**Source**
eIF2α		9722	rabbit	Cell Signalling
p-eIF2α	Ser 51	3398	rabbit	Cell Signalling
IRE1α	His963	3294	rabbit	Cell Signalling
JNK/SAPK		sc-571	rabbit	Santa Cruz
p-JNK/SAPK	Thr183/Tyr185	4668	rabbit	Cell Signalling
GAPDH		2118	rabbit	Cell Signalling
β-actin		A5441	mouse	Sigma
Akt		610861	mouse	BD Transduction Laboratories
p-Akt	Ser473	4060	rabbit	Cell Signalling
p-Akt	Thr308	2965	rabbit	Cell Signalling
IR		sc-711	rabbit	Santa Cruz
p-IR	Tyr1162/1163	sc-25103	rabbit	Santa Cruz

Supplementary Table 2: List of the primers used in PCR

Gene	RefSeq	Forward primer	Reverse primer
Acc-1	NM_133360	TGTCCGCACTGACTGTAACCA	TGCTCCGCACAGATTCTTCA
Atf4	NM_009716.2	CTCAGACAGTGAACCCAATTGG	GGCAACCTGGTCGACTTTTATT
Bim	NM_207680	AGGAGGGTGTTTGCAAATGATT	ACCAGACGGAAGATAAAGCGTAA
CD68	NM_009853	TGCGGCTCCCTGTGTGT	TCTTCCTCTGTTCCTTGGGCTAT
Chop	NM_007837.3	AGGAGCCAGGGCCAACA	TCTGGAGAGCGAGGGCTTT
Edem	NM_138677	GGATCCCCTATCCTCGGGT	GTTGCTCCGCAAGTTCCAG
Fasn	NM_007988	GATCCTGGAACGAGAACACGAT	AGAGACGTGTCACTCCTGGACTT
F4/80	NM_010130	GATGAATTCCCGTGTTGTTGGT	ACATCAGTGTTCCAGGAGACACA
Gadd34	NM_008654.2	TGGTCCAGCTGAGAATGAAGAG	GGAAGCAGCAGAAGCTTGGT
Grp78	NM_022310.2	AGCCATCCCGTGGCATAA	GGACAGCGGCACCATAGG
Hsp90	NM_011631	TGTTGTGGATTCCGATGATCTC	GCAATTTATGTTGCTGAAGAGTCTCA
Nqo1	NM_008706	CAATCAGCGTTCGGTATTACGA	GCCAGTACAATCAGGGCTCTTC
Pemt	NM_008819	GCGGCTGTGATCACCATTG	TCCCATCTCGCTACCACATTC
Rpl19	NM_009078	GAAGGTCAAAGGGAATGTGTTCA	CCTTGTCTGCCTTCAGCTTGT
Scd-1	NM_009127	CCAGAATGACGTGTACGAATGG	GCGTGTGTTTCTGAGAACTTGTG
Srebp1	NM_011480	CTGGCACTAAGTGCCCTCAAC	GCCACATAGATCTCTGCCAGTGT
Trib3	NM_175093	TGTCTTGCGCGACCTCAAG	CCAGCTTCGTCCTCTCACAGT
Xbp1*	NM_013842.2	ACACGCTTGGGAATGGACAC	CCATGGGAAGATGTTCTGGG

*PCR product loaded on a 3% agarose gel (spliced=147bp; unspliced=173bp)

Reference List

1. Lanthier,N., Molendi-Coste,O., Cani,P.D., van,R.N., Horsmans,Y. and Leclercq,I.A. (2011) Kupffer cell depletion prevents but has no therapeutic effect on metabolic and inflammatory changes induced by a high-fat diet. FASEB J. **25**, 4301-4311.

Supplementary Figure 1

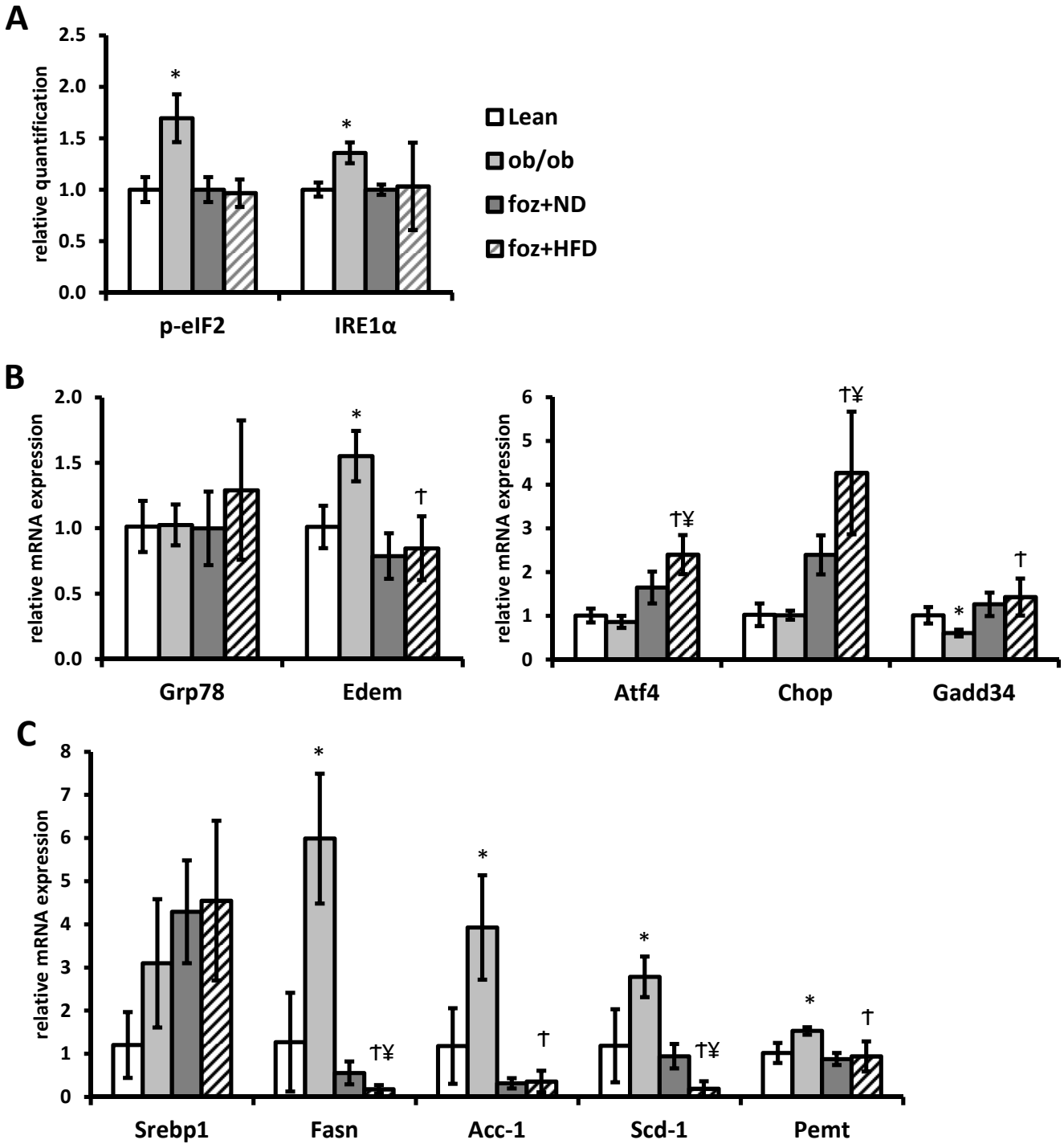

Supplementary Figure 2

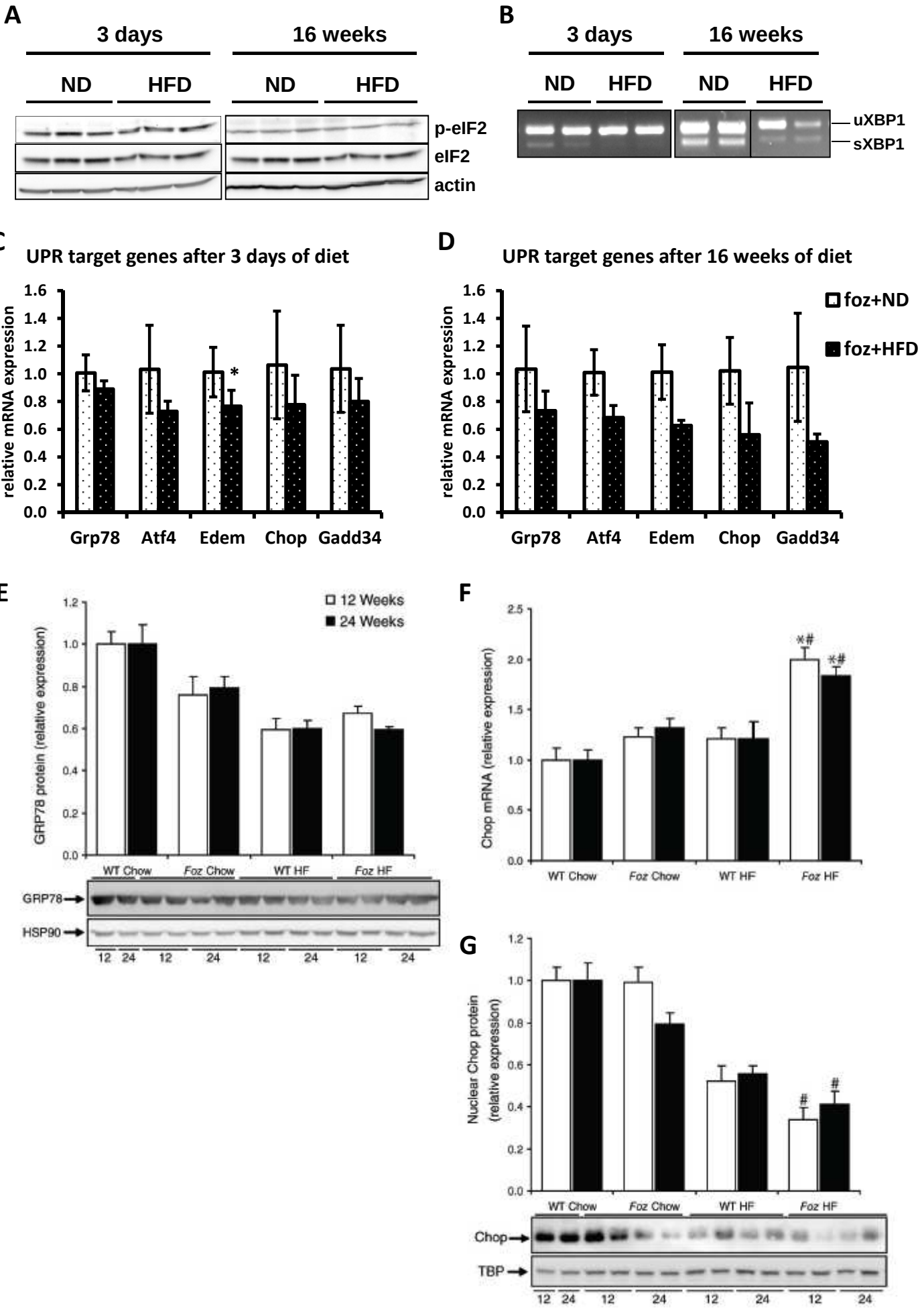

Supplementary Figure 3

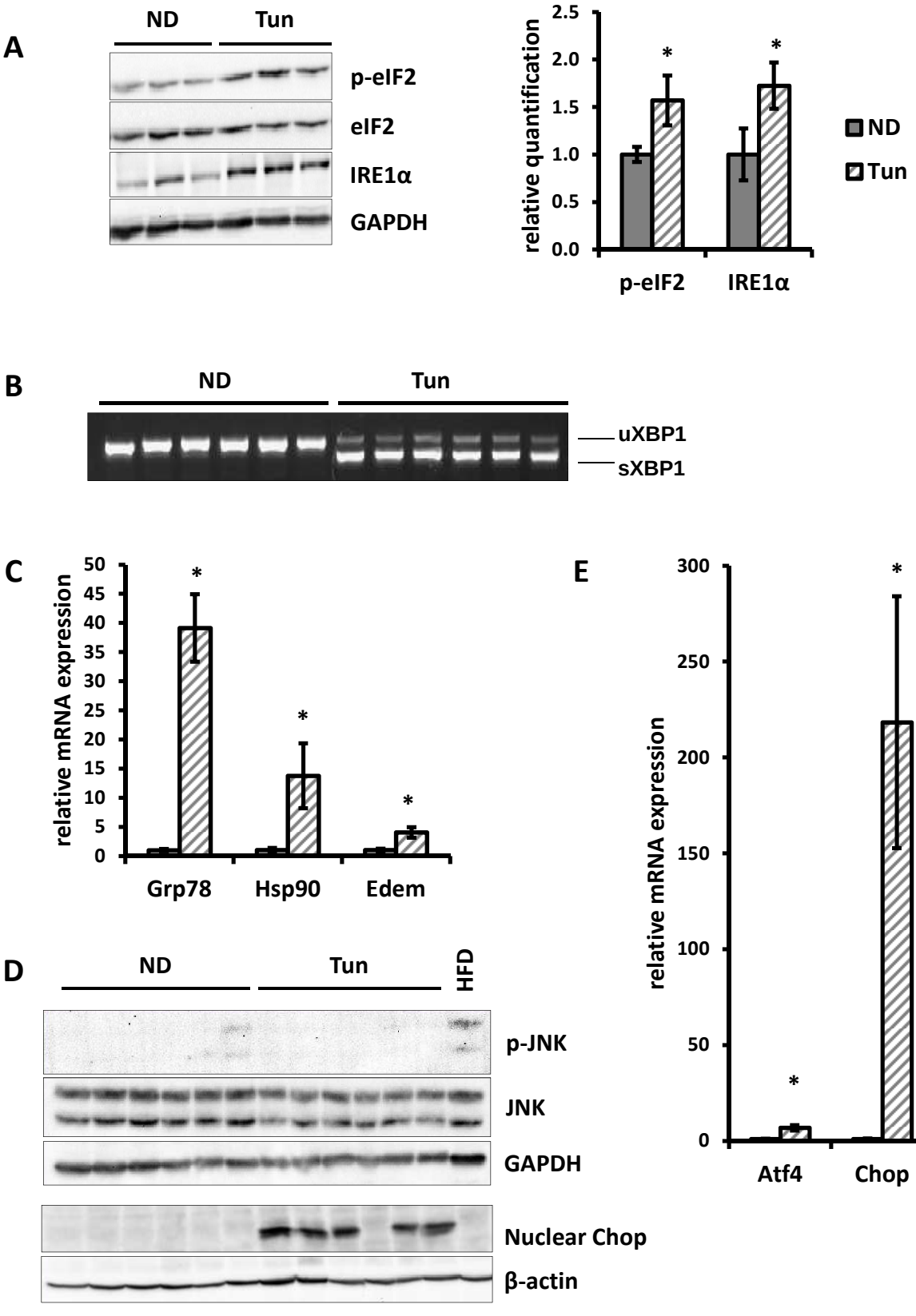

Supplementary Figure 4

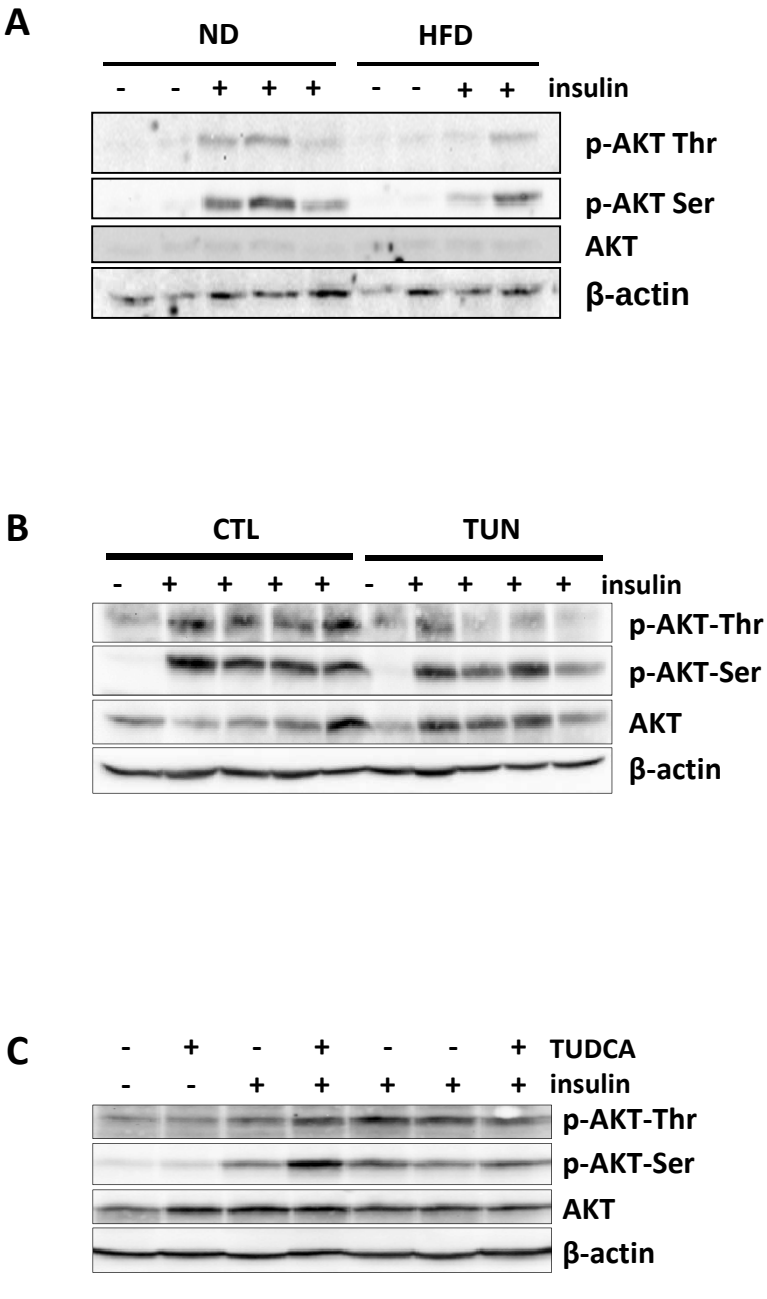

Supplementary Figure 5